

# Analysis and combination of different approaches for selective and directional thermal emission

Gerald Pühringer, Bernhard Jakoby

*Institute for Microelectronics and Microsensors, Johannes Kepler University Linz, Austria*  
 gerald.puehringer@jku.at

## Abstract

There are many concepts providing narrowband and highly directional mid-infrared (mid-IR) thermal emission for integrated sensor applications. In this contribution, we simulate the combination of two different concepts, each featuring individual signatures with respect to emission properties. The first concept is composed of an aperiodic multilayer stack of alternating dielectric layers (Si and SiO<sub>2</sub>) deposited on a planar metallic surface acting as heater ([1,2]). The dielectric double-layers either have quarter-wavelength (QW) thickness forming a Bragg mirror. This is followed by a half-wavelength (HW) cavity-layer of SiO<sub>2</sub> on top of a silver surface. The second concept is based on a structured silver surface, which utilizes the excitation of surface plasmon polaritons (SPPs) to gain the desired emission enhancement at the target wavelength ([3]). The very high coherence of the SPPs results in an extremely narrowband and directional emission. However, unwanted emission modes from SPP overtones can be a significant downside of this concept. We simulate and discuss the possibility of a combination of both concepts, which has the potential of keeping selective and high intensity emission properties without unwanted adjacent emission bands.

**Key words:** Thermal emitter, surface plasmon polaritons, Bragg-Mirror, mid-IR.

## Introduction

A radiation source yielding enough power in a specified narrow spectral range is highly desired for integrated optical IR absorption sensors. The vertical-cavity multilayer approach considered here faces several issues regarding the fabrication for devices optimized for the mid-infrared region. The reason for this lies in the emission characteristics, which are very sensitive to geometrical and optical properties of the material. The layer thicknesses demanded by mid-infrared light sources are posing a hard challenge to thin layer deposition techniques [4]. For this reason, it is favorable to reduce the number of dielectric layers involved in this approach. The thermal emitter concept based on the excitation of SPPs features even more narrowband high intensity emission at the target resonance wavelength, but also true for overtone emission modes in the spectral vicinity.

Here, we present a way of achieving a reduction of layer numbers as well as a suppression of the overtone emission by SPP excitation using the example of a target mid-IR emission wavelength of  $\lambda=4.26\ \mu\text{m}$ .

## Simulations

By Kirchhoff's law ([1,3,5]), the absorbed power of a surface is closely related to its emissive properties at thermal equilibrium. The simulations utilize this principle by calculating the absorption of incoming light at different wavelengths in order to characterize the emissive behavior of the structure by virtue of the reciprocity underlying Kirchhoff's law. If there is no absorption at the boundaries and no transmission, the energy fraction  $\alpha$  absorbed by the metal (here Ag) is determined by

$$\alpha = 1 - r, \quad (1)$$

where  $r$  is the reflected amplitude from the incoming port.

Figures 1 and 2 depict two different configurations considered in this work, one with periodic and one with absorbing boundary conditions at the side walls. The former features an incoming TM polarized plane wave at the input port boundary, while the latter features an incoming guided TM polarized slab mode. The numerical calculations are performed by using the commercial software COMSOL Multiphysics, which is based on finite element methods (FEM).

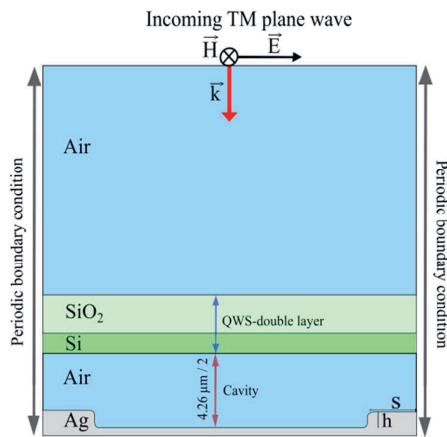


Fig. 1. Periodic configuration with one dielectric QWS double layer and a structured metal on the bottom. A TM polarized plane wave enters the structure vertically ( $\theta=0$ ). The air cavity length is a half of the target absorption wavelength. The grating profile is determined by the parameters  $s$  and  $h$ .

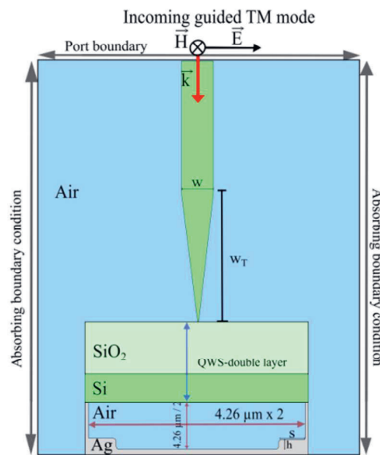


Fig. 2. Configuration with absorbing side walls. An incident guided TM slab mode from the top is coupled via an inverse taper to the cavity, which confines light in  $x$ - and  $y$ - direction.

### Material Properties

As the thermal emitter structures are designed for the mid-infrared spectral region, the optical constants of Si, SiO<sub>2</sub> and Ag were modeled for an operating temperature of  $\sim 800$  K. The procedure to achieve this is given in [1,6–8].

### Lumped Parameter Model

[1], [9] and [3] give a model using lumped parameters and perturbation theory to describe the absorption mechanism by coupling light into a resonant cavity mode. The result of this analysis is that the absorption (or the coupling into the cavity) is maximized if the loss rate in the cavity due to internal material absorption  $P_{int}$  matches the loss rate to far-field radiation  $P_{ext}$ , thus  $P_{int} = P_{ext}$  at resonance.

This model can be applied to both thermal emitter concepts (VERTE and SPP-grating).

For the VERTE,  $P_{int}$  is determined by the choice of the plane metal and  $P_{ext}$  by the number of dielectric quarter-wave double layers. The SPP-grating determines these quantities by tuning the geometry of the grating profile (i.e. height and width of grating sites). 100 % absorption is achieved for both concepts if the loss rates match at resonance.

Having a plasmonic grating structure together with a dielectric reflective mirror, a confinement in both dimensions can now be achieved in the cavity for the 2D problem. The simple configuration discussed here is the addition of two quarter-wave dielectric layers at half-wave distance to the metal surface. Readjusting the grating profile now again allows to rematch  $P_{int}$  and  $P_{ext}$  in order to achieve again 100% absorption. We will see that this approach has the potential of reducing the intensity of strong plasmonic overtone absorption mode.

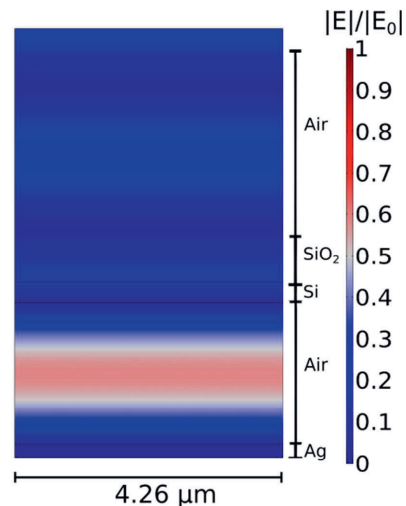


Fig. 3. Electric field distribution of a multilayer emitter with only two dielectric layers and no grating structure in the silver substrate. The low electric field leads to a weak enhancement of the emissivity (red line in figure 4).

### Periodic boundary conditions and two dielectric layers

Applying periodic boundary conditions at the sides allows to use (1) to determine the total absorption of the structure. A plane wave incoming from the top port boundary gets weakly absorbed creating a slightly enhanced electric field, as can be seen in Fig. 1. By increasing the number of double-layers  $P_{ext}$  can be reduced in order to achieve near unity absorption [1]. Similarly,  $P_{int}$  can be enhanced by SPP-excitation, which is the situation simulated in this work.

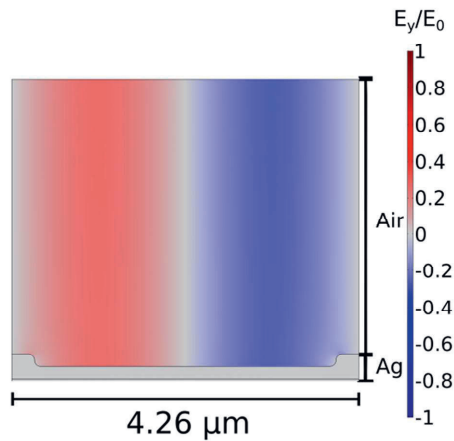


Fig. 4. Field distribution of an plasmonic emitter (no dielectric layers, corresponding to black line in Fig. 7), see [3].

### Excitation of plasmons

With an optimized grating profile, the total electric field gets vertically scattered by the grating and strongly enhanced by SPPs. It is demonstrated in [3] that highly coherent and directional emission with bandwidths below 1 nm can be achieved with this approach. However, the high SPP-coherence of the also leads to strong emission bands at overtone frequencies of the target emission frequency. With an additional confinement of the electric field in y-direction and a readjustment of the grating profile, it should be possible to maintain the absorption performance at the target emission wavelength, while suppressing the absorption at the overtone frequencies. We observe a strong enhancement of the emissivity compared to the configuration with plane silver, which dominates the much weaker field confinement in y-direction (Fig. 2). Nevertheless, there are some key differences compared to the plasmon-only field confinement configuration (Fig. 5): First, the bandwidth is not as narrow and, second, overtone emission modes show far less intensity. Furthermore, the overtone modes feature a different quantity and occur at different resonance frequencies. This shows SPP supported cavity mode can be created, which also results in strong enhancement of the absorption in the metal. However, the quality factor of the cavity declined compared to the configuration without the dielectric double-layers, as reflected by the broadened bandwidth.

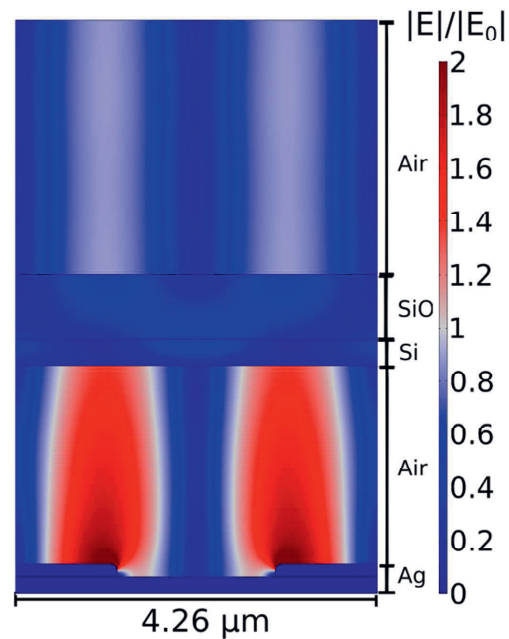


Fig. 5. Field distribution of the configuration in Fig. 1 with optimized geometry for maximum absorption/emission at resonance wavelength (see blue line in figures 6 and 7).

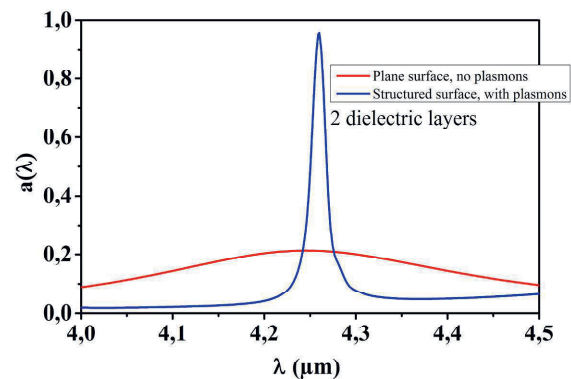


Fig. 6. Absorption of multilayer emitters consisting of only two dielectric layers. For plane silver, the enhancement of the emission is very low and broadband (red line, corresponding to figure 3). A properly structured silver surface (supporting the excitation of resonant SPPs) can enhance the electric field and the absorption (see figure 3).

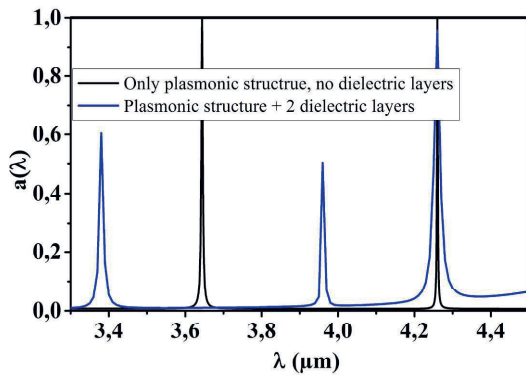


Fig.7 Absorption in a larger spectral window compared to figure 6. The configuration without dielectric layers (see figure 4) exhibits strong overtone absorption at  $\sim 3.7 \mu\text{m}$  (black line). With dielectric layers (blue line) the intensities are suppressed by  $\sim 40\text{-}50\%$ .

### Coupling to a finite cavity via inverse taper

This section should demonstrate a the possibility to couple light from a waveguide mode into a cavity confining light in both dimensions with absorbing instead of periodic boundary conditions at the side walls. Here, the coupling is performed by an inverse taper, which is one of the simplest ways of achieving efficient mode-coupling (see figure 2). The narrowing of the waveguide width leads to a widening of the mode width ([10,11]), which leads to a matching with the cavity mode profile width. The reflective metal sidewalls form a pseudo-periodic boundary in x-direction. The width of the cavity is now two times the target resonance absorption wavelength. Thus, the first SPP overtone is excited. This allows an enlargement of the cavity, while applying a grating profile only at its edges. The width and the height of the grating profile was again readjusted to maximize the total field absorption in the cavity (i.e. matching  $P_{\text{int}}$  to  $P_{\text{ext}}$ ). However, (1) is not valid anymore, as a significant fraction of the incoming guided light is scattered by the dielectric double layers into the air region and absorbed by the boundary conditions at the side walls. Thus, efficient coupling into the cavity remains a problem to be solved.

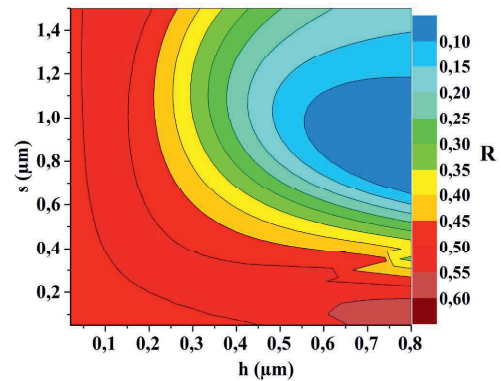


Fig.8 Contour plot showing different reflection amplitudes with varying the grating parameters  $s$  and  $h$ . The red region shows fairly high reflectance back into the waveguide port, while the blue region features SPP-excitation and minimizes the reflections.

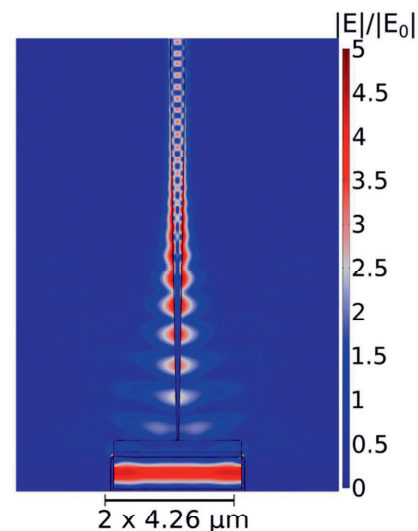


Fig.9 Field distribution of the configuration in Fig.2 featuring no SPP-excitation (corresponding to red region in figure 6). The fairly high intensity in the cavity and in the waveguide region can be seen. However, a significant fraction gets scattered in the air region.



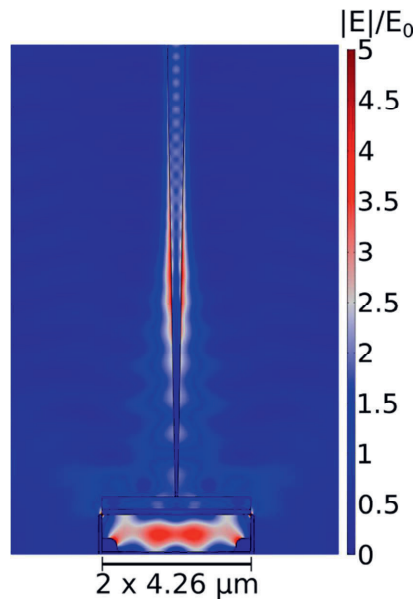


Fig.10 Field distribution of the configuration in Fig.2 featuring SPP-excitation (corresponding to blue region in figure 6). The fairly low intensity in the waveguide region can be seen. The total electric field results from an overlap between the two field enhancing mechanisms.

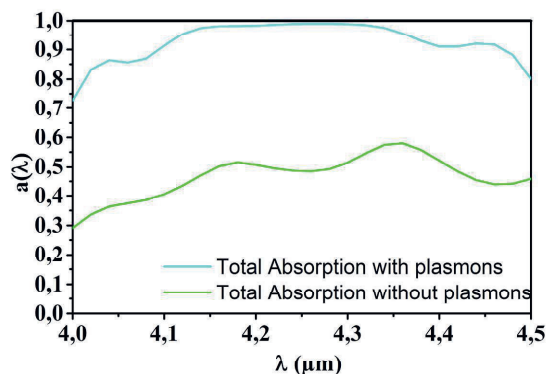


Fig.11 Absorption for the non-periodic configuration in with (light blue line) and without (light green line) SPP excitation. The broadband absorption is due to scattering in the air region and a low cavity quality factor.

Figure 8 shows the sensitivity of the reflection with respect to the geometrical parameters of the grating profile. The region with minimum reflection corresponds to the region which features SPP-excitation, which can be directly seen by the shape of the E-field in figure 10 in the cavity region. The red region corresponds to cavity modes without SPPs (figure 9). Here, the field is much stronger in the waveguide region, which reflects the larger amplitude of the reflected guided mode.

However, a significant fraction of the incoming light is scattered into the air region and subsequently absorbed by the boundary conditions at the side walls. Nevertheless, figure 9 and 10 demonstrate significant field

enhancement and subsequently coupling into the cavity. At least, this shows that a fraction of light can be coupled into the waveguide if a field in the cavity is created by thermal emission in the time-reversed picture. Figure 11 shows that the absorption occurs at a broader spectral range compared to the configuration with periodic boundary conditions. This is a consequence of the worsened quality factor of the cavity and the scattering losses to the air region.

## Conclusions

In this work we demonstrated the possibility to combine different concepts to achieve selective thermal emission in the mid IR region. The periodic configuration showed that unity resonant absorption can be achieved again by creating unique cavity modes, which exacerbate the fulfilling of the resonance condition at overtone frequencies. Figure 7 shows the suppressing of the intensities of the overtone absorption modes.

Furthermore, we showed coupling between a finite cavity and slab waveguide mode. The finite cavity now utilizes SPP overtones for achieving unique cavity modes. The high SPP-coherence length allows increasing the cavity length in x-direction in a simple manner. Efficient coupling to the unique cavity mode remains an issue to be solved. Grating couplers are the most promising candidates for achieving this, as these can be optimized for coupling between arbitrary propagation modes in flexible manner.

## Acknowledgement

This work has been supported by the COMET K1 centre ASSIC Austrian Smart Systems Integration Research Center. The COMET – Competence Centers for Excellent Technologies- Programme is supported by BMVIT, BMWFW and the federal provinces of Carinthia and Styria.

## References

- [1] I. Celanovic, D. Perreault, J. Kassakian, Resonant-cavity enhanced thermal emission, *Phys. Rev. B.* 72 (2005) 2–7. doi:10.1103/PhysRevB.72.075127.
- [2] G. Pühringer, B. Jakoby, Modeling of a Highly Optimizable Vertical-Cavity Thermal Emitter for the Mid-Infrared, *Procedia Eng.* 168 (2016) 1214–1218. doi:10.1016/j.proeng.2016.11.419.
- [3] L. Meng, D. Zhao, Z. Ruan, Q. Li, Y. Yang, M. Qiu, Optimized grating as an ultra-narrow band absorber or plasmonic sensor., *Opt. Lett.* 39 (2014) 1137–40. doi:10.1364/OL.39.001137.

- [4] M. Knapp, J. Philipp, W. Ruile, I. Bleyl, L.M. Reindl, A refined method to determine the elastic constants of SiO<sub>2</sub> thin films, (2014) 277–280.
- [5] V. Shklover, L. Braginsky, G. Witz, M. Mishkirey, C. Hafner, High-Temperature Photonic Structures. Thermal Barrier Coatings, Infrared Sources and Other Applications, *J. Comput. Theor. Nanosci.* 5 (2008) 1–32. doi:10.1166/jctn.2008.003.
- [6] K. Ujihara, Reflectivity of metals at high temperatures, *J. Appl. Phys.* 43 (1972) 2376–2383. doi:10.1063/1.1661506.
- [7] J. Kischkat, S. Peters, B. Gruska, M. Semtsiv, M. Chashnikova, M. Klinkmüller, O. Fedosenko, S. Machulik, A. Aleksandrova, G. Monastyrskyi, Y. Flores, W.T. Masselink, Mid-infrared optical properties of thin films of aluminum oxide, titanium dioxide, silicon dioxide, aluminum nitride, and silicon nitride, *Appl. Opt.* 51 (2012) 6789–6798. doi:10.1364/AO.51.006789.
- [8] H.H. Li, Refractive index of silicon and germanium and its wavelength and temperature derivatives, 1979.
- [9] D.H. Staelin, *Electromagnetics and Applications*, (2011) 1–442.
- [10] A. Mekis, J.D. Joannopoulos, Tapered couplers for efficient interfacing between dielectric and photonic crystal waveguides, *J. Light. Technol.* 19 (2001) 861–865. doi:10.1109/50.927519.
- [11] L. Chen, C.R. Doerr, Y.K. Chen, T.Y. Liow, Low-loss and broadband cantilever couplers between standard cleaved fibers and high-index-contrast Si<sub>3</sub>N<sub>4</sub> or Si Waveguides, *IEEE Photonics Technol. Lett.* 22 (2010) 1744–1746. doi:10.1109/LPT.2010.2085040.